

Research Article

Macroscopic Balance Equations for Spatial or Temporal Scales of Porous Media Hydrodynamic Modeling

Shaul Sorek* and Yuval Ohana

The Department of Environmental Hydrology & Microbiology, Ben-Gurion University of the Negev, Israel

***Corresponding author:** Shaul Sorek, J. Blaustein Institutes for Desert Research, Zuckerberg Institute for Water Research, Environmental Hydrology & Microbiology, Ben-Gurion University of the Negev, Midreshet Ben-Gurion 84990, Israel

Received: June 24, 2014; **Accepted:** November 26, 2014; **Published:** January 23, 2015

Abstract

We focus on the first author's previous work addressing macroscopic balance equations developed for different spatial and temporal scales. We elaborate on previous findings so as to orient the reader to fundamental concepts with which the mathematical formulations are developed. The macroscopic balance Partial Differential Equations (PDE's) are obtained from their microscopic counterparts by volume averaging over a Representative Elementary Volume (REV), considering a non-Brownian motion. The macroscopic quantity of phase/component intensive quantities product, is the premise of two concurrent decomposed macroscopic balance PDE's of the corresponding extensive quantity. These are concurrently valid at the primary REV order of length and at a significantly smaller secondary length. The hydrodynamic characteristic at the smaller spatial scale was found to always be described by pure hyperbolic PDE's, the solution of which presents displacement of sharp fronts. Reported field observations of condensed colloidal parcels motion, validate the suggestion of hyperbolic PDE's describing fluid momentum and components mass balance at the smaller spatial scale. Controlled experiments supplemented by numerical predication can yield the hydrodynamic interrelation between the two adjacent spatial scales.

Further, we focus on the first author past developments concerning dominant macroscopic balance PDE's of a phase mass and momentum and a component mass following an onset of abrupt pressure change. These account for the primary REV order of length and for evolving temporal scales. Numerical simulations were found to be consistent in excellent agreement with experimental observations. During the second time increment and in view of the aforementioned developments, we presently elaborate on new findings addressing theoretically the efficiency of expansion wave for extracting solute from a saturated matrix. Simulations comparing between pumping using an approximate analytical form based on Darcy's equation and numerical prediction addressing the emitting of an expansion wave, suggest that the latter extracts by far more solute mass for a spectrum of different porous media.

Keywords: Averaging over a Representative Elementary Volume (REV); Deviation from REV spatial average; Primary and secondary macroscopic balance equations; Temporal approximate primary balance equations; Forchheimer's momentum term

Introduction

Application of spatial averaging rules, referring to a REV, leads to the formulation of the macroscopic balance equations addressing phase interactions such as fluids carrying components and a deformable porous matrix [1]. Further elaborations by Sorek et al. [2], Sorek and Ronen [3] and Sorek et al. [4], prove that the phases and components macroscopic balance PDE's can be decomposed into a primary part that refers to the REV length scale and, concurrently, a secondary part valid at a length scale smaller than that of the corresponding REV length. The secondary macroscopic balance equation always conforms to a hyperbolic PDE. Geometrical patterns of different spatial scales that prevail in various porous media are exemplified in Figure 1. Such patterns support the notion of the need to implement macroscopic balance equations addressing different spatial scales. Observations [4] verify that the hydrodynamic

characterization of colloidal transport comply with the developed fluid and component macroscopic balance equations for the smaller spatial scale.

Accounting for the primary macroscopic phase/component balance PDE's at the larger REV scale and neglecting the secondary ones, one can study their approximate dominant forms obtained at evolving time scales. It was shown [5] that during a certain time period, following an abrupt pressure rise, the Newtonian fluid momentum balance equation conforms to a nonlinear wave equation. Following sorek et al. Sorek et al. [6] Sorek et al. and Levy et al. [7], the exchange of microscopic inertia through the solid-fluid interface in the form of Forchheimer terms were introduced [8] and extended [2], resulting in a variety of nonlinear wave equation forms.

In case of a Newtonian fluid, Sorek et al. [2] refer to the fluid momentum balance equation and obtain extended forms of the

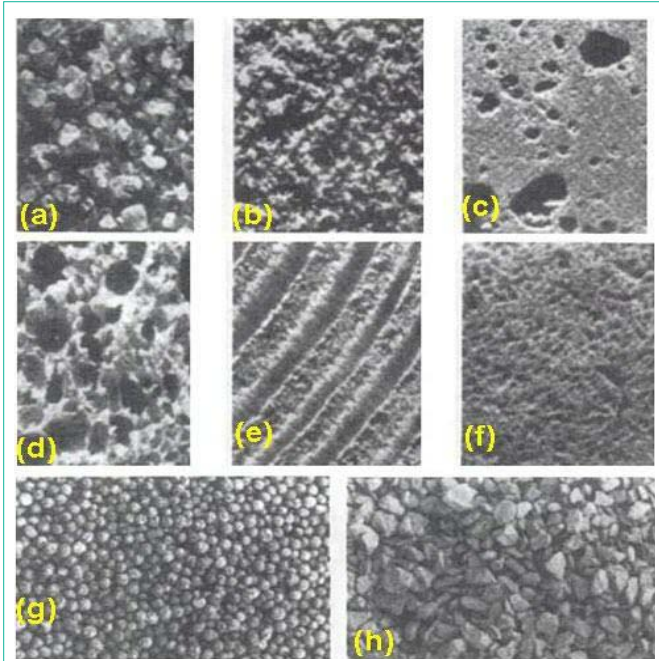


Figure 1: Examples of porous materials: (a) Beach sand; (b) Sandstone; (c) Limestone; (d) Rye bread; (e) Wood; (f) Human lung; (g) Spheres packing for granular structures; (h) Crushed limestone for construction. (After D. A. Nield and A. Bejan, "Convection in Porous Media", Springer, 2006).

macroscopic Navier-Stokes (NS) equation. These at the REV scale can vary from inertia fluxes in the form of a nonlinear wave equation, Forchheimer’s law expressing the transmittance of fluid inertia to the solid matrix through their microscopic solid-fluid interface, or conform to Darcy’s law when friction at that interface is dominant.

Spatial Scaling of the General Macroscopic Balance Equations

Addressing Bear and Bachmat (1990) the spatial averaging over the volume, $U_{0\alpha}$, of the α phase within the, U_0 , REV volume dictates the relations,

$$\bar{e}^\alpha = e_1 e_2^\alpha = e_1^\alpha e_2^\alpha + e_1 e_2^\alpha; e_1 + e_2^\alpha = e_1^\alpha + e_2^\alpha, \tag{1}$$

Where $\bar{e}_i^\alpha (\equiv \frac{1}{U_{0\alpha}} \int e_i dU)$ denotes the i intensive macroscopic quantity of the α phase, spatially averaged over $U_{0\alpha}$ and $e_i^\alpha (\equiv e_i - \bar{e}_i^\alpha)$ denotes its deviation from \bar{e}_i^α . The Left Hand Side (LHS) of can, e.g., refer to the microscopic phase extensive quantity (E) being the momentum ($\mathbf{E} \equiv \mathbf{M}$) vector (i.e. $e^M = \rho \mathbf{V}$; $e_1 \equiv \rho$ phase density; $e_2 \equiv \mathbf{V}$ phase velocity vector).

Modified rule (Bear and Bachmat, 1990) for averaging a spatial derivative reads

$$\frac{\partial \bar{e}^\alpha}{\partial x_i} \equiv \frac{\partial \bar{e}^\alpha}{\partial x_j} T_{aj}^* + \frac{1}{\theta_\alpha U_0} \int_{S_{\alpha\beta}} x_i \frac{\partial e}{\partial x_j} \xi_j ds, T_{aj}^* \equiv \frac{1}{\theta_\alpha U_0} \int_{S_{\alpha\alpha}} x_i \xi_j ds, \tag{2}$$

where \mathbf{x} denotes a distance vector from the REV centroid to the microscopic interface surface ($S_{\alpha\beta}$) between the α and β phases, $\theta_\alpha \equiv U_{0\alpha}/U_0$ denotes the volume ratio associated with the α phase, $\bar{e}^\alpha = \theta_\alpha \bar{e}^\alpha$ with $\bar{e}^\alpha (\equiv \frac{1}{U_0} \int e dU)$ denoting average of the α phase over a REV, ξ denotes a unit vector outward to an interface and \mathbf{T}_α^* denotes the α phase tortuosity tensor associated with ($S_{\alpha\alpha}$) the α - α part of the REV enclosing interface.

Note that for $\mathbf{E} \equiv U_{0\alpha}$ we obtain $e (\equiv dE/dU_{0\alpha}) = 1$ for which $\bar{e}^\alpha = 1$ leading to $\bar{e} = \theta_\alpha$. While (2) is authenticated, the non-modified rule $\frac{\partial \bar{e}^\alpha}{\partial x_i} \equiv \frac{\partial \bar{e}^\alpha}{\partial x_j} + \frac{1}{U_0} \int_{S_{\alpha\beta}} \xi_j ds$ for averaging a spatial derivative, when $\mathbf{E} \equiv U_{0\alpha}$, results with the relation $\frac{\partial \bar{e}^\alpha}{\partial x_i} = -\frac{1}{U_0} \int_{S_{\alpha\beta}} \xi_i ds$.

In [2-4] it was assumed that:

Assumption 1 [A.1] The microscopic interface surface between two adjacent phases is material to the extensive quantity flux of the phases.

Assumption 2 [A.2] The phase intensiveness, e , quantity accounts for a high Strouhal number $St \gg 1$ $St \equiv \frac{L_c / t_c}{V_c}$, with characteristic quantities L_c, t_c, V_c of length, time and phase velocity, respectively).

We note that by virtue of [A.2], the hydrodynamic derivative of a macroscopic quantity can be approximated by its corresponding temporal derivative at a fixed frame of reference, and together with [A.1] it is replaced by the macroscopic temporal derivative (i.e., $\frac{D\bar{e}^\alpha}{Dt} \equiv \frac{\partial \bar{e}^\alpha}{\partial t} = \frac{\partial \bar{e}^\alpha}{\partial t}$, respectively).

In view of (1), [A.1], [A.2] and elaborating on Bear and Bachmat (1990), the general macroscopic balance equation of a phase extensive (E) quantity reads,

$$\frac{\partial}{\partial t} [\theta_\alpha (\bar{e}_1^\alpha \bar{e}_2^\alpha + e_1 e_2^\alpha)] = -\nabla \cdot [\theta_\alpha (\bar{e}_1^\alpha \bar{e}_2^\alpha + e_1 e_2^\alpha) \bar{\mathbf{V}}^\alpha + \theta_\alpha (e \bar{\mathbf{V}}^\alpha + \mathbf{J}^E)] + \theta_\alpha \rho \Gamma^E \tag{3}$$

in which $\bar{\mathbf{V}}^\alpha$ denotes its macroscopic velocity vector, $\mathbf{J}^E (\equiv e(\bar{\mathbf{V}}^\alpha - \mathbf{V}^\alpha))$ denotes the macroscopic diffusive flux vector obtained by empirical relation, habitually, following a potential flux pattern Γ^E denotes the rate of generating the phase extensive quantity per its unit mass. Note that (3) accounts for $\bar{\mathbf{e}}^\alpha \bar{\mathbf{V}}^\alpha \equiv \bar{e}^\alpha \bar{\mathbf{V}}^\alpha + e_1 e_2^\alpha \bar{\mathbf{V}}^\alpha$ the macroscopic flux vector of the phase extensive quantity which is decomposed into the advective flux ($\bar{e}^\alpha \bar{\mathbf{V}}^\alpha$), the dispersive flux ($e_1 e_2^\alpha \bar{\mathbf{V}}^\alpha$) and $e_1 e_2^\alpha \bar{\mathbf{V}}^\alpha$ that accounts for the deviation from the advective flux. Supplement to [1] and following [4], we write,

Assumption 3 [A.3] Phase motion is not of a Brownian type, as the vanishing of its macroscopic intensive quantity will cause the disappearance of the deviation from that intensive quantity (i.e. $\bar{e}^\alpha = 0 \Rightarrow \bar{e}^\alpha = 0$, iff $e = 0$).

Hereinafter, for the sake of reducing the overload of notations, we will refer to the α phase macroscopic quantities without the $(\bar{\cdot})^\alpha$ [$\equiv \frac{1}{U_{0\alpha}} \int (\cdot) dU$] designator.

By the premise of [A.3], in terms of the α phase macroscopic quantities for any spatial scale, we write

$$\bar{e}^\alpha = \Lambda_E e \tag{4}$$

in which Λ_E denotes a factor (e.g. obtained empirically) that, depending on the e quantity, can be a scalar, an element of a vector or of a tensor. By virtue of (4) we can thus relate the dispersive flux in (3) to the advective flux, reading

$$\bar{e}^\alpha \bar{\mathbf{V}}^\alpha = \mathbf{A} \cdot e \mathbf{V}, \mathbf{A} = \Lambda_E \mathbf{\Lambda}_V; \bar{\mathbf{V}}^\alpha = \mathbf{\Lambda}_V \cdot \mathbf{V}, \tag{5}$$

where $\mathbf{\Lambda}_V$ is a tensor quantity. Addressing (3), the phase macroscopic quantity of the product of deviations from their corresponding intensive quantities (in what follows denoted by d^E) can by virtue of (4) be related to the product of their macroscopic

quantities,

$$d^E \equiv e_1 \cdot e_2 = \Lambda_{e_{12}} e_1 e_2, \Lambda_{e_{12}} \equiv \Lambda_{e_1} \Lambda_{e_2} \cdot \tag{6}$$

Referring to (3) we can make an assumption that addresses the deviation from the advective flux.

Assumption 4[A.4] *The product of intensive quantities is dominant over that of their corresponding deviations* $|e_1 e_2| \gg |e_1 \cdot e_2|$.

As by virtue of (6) we have $|e_1 e_2| = |\Lambda_{e_{12}} e_1 e_2|$, the [A.4] assumption leads to $\varepsilon_\alpha \equiv |\Lambda_{e_{12}}| \ll 1$ from which we obtain $\Lambda_{e_{12}} = \varepsilon_\alpha B_e, |B_e| = 1$.

On the premise of (6) and [A.4], we rewrite (3) as a balance equation addressing the advective, dispersive and diffusive fluxes, the assumed smaller term associated with deviation from the intensive quantity ($\varepsilon_\alpha \theta B_e e_1 e_2$) and its corresponding assumed smaller term of deviation from the advective flux ($\varepsilon_\alpha \theta B_e e_1 e_2 \mathbf{V}$),

$$\frac{\partial}{\partial t}(\theta e_1 e_2) + \varepsilon_\alpha \frac{\partial}{\partial t}(\theta B_e e_1 e_2) = -\nabla \cdot [\theta(e_1 e_2 \mathbf{V} + e_1 \cdot e_2 \mathbf{J}^E)] + \theta \rho \Gamma^E - \varepsilon_\alpha \nabla \cdot (\theta B_e e_1 e_2 \mathbf{V}). \tag{7}$$

Referring to (3), different forms of balance equations will emanate subject to assumptions made when comparing between decompositions of the phase extensive quantity flux $e \mathbf{V}^E [= e \mathbf{V} + e_1 \cdot e_2 \mathbf{J}^E]$ (e.g. neglecting the momentum dispersive flux, when addressing medium heterogeneity). Let us thus consider the assumption that,

Assumption 5[A.5] *The advective flux is dominant over the dispersive flux* $|e \mathbf{V}| \gg |e_1 \cdot e_2 \mathbf{J}^E|$. As by virtue of (5) we have $|e_1 \cdot e_2 \mathbf{J}^E| = |\Lambda_{e_{12}} e \mathbf{V}|$, the [A.5] assumption leads to $\varepsilon \equiv |\Lambda_{e_{12}}| \ll 1$ so that $\mathbf{A} = \varepsilon \mathbf{B}, \|\mathbf{B}\| = 1$.

On the premise of (5), [A.4] and [A.5] we rewrite (3) as a balance equation addressing the advective and diffusive fluxes, the assumed smaller term associated with deviation from the intensive quantity and the assumed smaller terms of deviation from the advective flux and the dispersive flux ($\theta(\varepsilon_\alpha B_e \mathbf{I} + \varepsilon \mathbf{B}) \cdot e_1 e_2 \mathbf{V}$),

$$\frac{\partial}{\partial t}(\theta e_1 e_2) + \varepsilon_\alpha \frac{\partial}{\partial t}(\theta B_e e_1 e_2) = -\nabla \cdot [\theta(e_1 e_2 \mathbf{V} + \mathbf{J}^E)] + \theta \rho \Gamma^E - \nabla \cdot [\theta(\varepsilon_\alpha B_e \mathbf{I} + \varepsilon \mathbf{B}) \cdot e_1 e_2 \mathbf{V}], \tag{8}$$

where \mathbf{I} denotes the unit tensor.

As both solutions of (7) and (8) when $\varepsilon \approx 0(\varepsilon_\alpha)$ are functions of $\varepsilon \ll 1$, we can expand their dependent variables using terms associated with a polynomial of ε powers. Approximate solutions to (7) and (8) can thus be obtained by solving an infinite set of the corresponding balance equations of descending order magnitudes. While the first (i.e. when $\varepsilon = 0$) balance equation may be nonlinear and of the highest order of magnitude, the others are linear balance equations as they are combined with variables obtained from the solution of equations that are of higher order magnitude. In view of (7) we hence obtain the *general primary (dominant) macroscopic balance equation for any α phase* corresponding to the REV (larger) length scale in the form of

$$\frac{\partial}{\partial t}(\theta e_1 e_2) = -\nabla \cdot \left[\theta \left(e_1 e_2 \mathbf{V} + e_1 \cdot e_2 \mathbf{J}^E \right) \right] + \theta \rho \Gamma^E \tag{9}$$

for which the combined, respectively, dispersion and diffusion fluxes ($e \mathbf{V} + \mathbf{J}^E$) habitually follow a macroscopic extension suggested for the empirical microscopic law associated with \mathbf{J}^E . This commonly has the pattern of a potential flow, and thus (9) conforms to a PDE with hyperbolic or parabolic characteristics.

By virtue of (6) we obtain the equation of a lesser order of

magnitude than (9), i.e. the *secondary macroscopic balance equation* emerging from (7) and assumed to correspond to a length span much smaller than that of (9), reads

$$\frac{\partial}{\partial t}(\theta d^E) = -\nabla \cdot (\theta d^E \mathbf{V}). \tag{10}$$

We note that (9) and (10) are based on a different premise and thus can represent different characteristics. At the REV (larger) spatial scale and subject to different assumptions, the governing balance equation (9) can accommodate pure advection, advection – dispersion or pure dispersion fluxes. The secondary governing balance equation (10) describes the concurrent pure advection (i.e. hyperbolic PDE characterized by a sharp front migration of the state variable) of the deviation (d^E) from the intensive quantity and its corresponding deviation from the advective flux, at a spatial scale much smaller than that of the REV. The solution for d^E of (10) depends also on \mathbf{V} , obtained from the solution of (9). Moreover, one can seek further resolution modes of d^E and \mathbf{V} , via an iterative process between (10) and the combined form of (9) and (10) [i.e. the original form of (7)].

By virtue of [A.5], another possible form emanating from (8) is a *general primary (dominant) macroscopic balance equation for any α phase* valid at the REV (larger) length scale that reads

$$\frac{\partial}{\partial t}(\theta e_1 e_2) = -\nabla \cdot \left[\theta \left(e_1 e_2 \mathbf{V} + \mathbf{J}^E \right) \right] + \theta \rho \Gamma^E \tag{11}$$

By virtue of (8), for $\varepsilon \approx 0(\varepsilon_\alpha)$ and on the basis of (8), concurrent to (11) yet with a smaller order of magnitude and at a length span much smaller than the typical length scale of the REV, the *secondary macroscopic balance equation for any α phase* reads

$$\frac{\partial}{\partial t}(\theta d^E) = -\nabla \cdot \left\{ \theta \left[\mathbf{I} + (\Lambda_{e_{12}})^{-1} \mathbf{A} \right] \cdot d^E \mathbf{V} \right\} \tag{12}$$

We note that unlike (10) and by virtue of [A.5], deviation from the advective flux ($e_1 e_2 \mathbf{V}$) and the dispersive flux ($e \mathbf{V}$), both assumed smaller than the advective flux ($e_1 e_2 \mathbf{V}$), are accounted for in (12). The discussion and procedure referring to (7), (9) and (10) corresponds, respectively, also to (8), (11) and (12). Sorek et al. [4] demonstrate the form and validity of the implication of (9) and (10) its corresponding secondary balance equation, as well as (11) and (12) its corresponding secondary balance equation. These two fundamental group forms (9), (10) and (11), (12), address, respectively, in [4] the balance equations of a component mass transport and phase energy (accounting for the advective and dispersive fluxes, when addressing their larger scale) and phase momentum (neglecting its dispersive flux for its larger scale).

Spatial scaled momentum balance equations of a phase

Following [2,4], here the phase extensive quantity is its momentum (i.e. $\mathbf{E} \equiv \mathbf{M}$), for which its macroscopic quantities are $e^M \equiv \rho \mathbf{V}$ (i.e. $e_1^M \equiv \rho e_1 \mathbf{V} \equiv \rho \mathbf{V}$), the momentum diffusive flux $\mathbf{J}^M = -\boldsymbol{\sigma}$ ($\boldsymbol{\sigma}$ -phase stress tensor) and the momentum source flux $\Gamma^M = \mathbf{F}$ (\mathbf{F} - specific body force acting on the phase). Following (6) and [A.4] we consider that $|e \mathbf{V}| \gg |e_1 \cdot e_2 \mathbf{J}^E|$. Thus, by virtue of (11), the *primary macroscopic momentum balance equation* of the α phase at the larger spatial scale of the typical REV length reads

$$\frac{\partial}{\partial t}(\theta \rho \mathbf{V}) = -\nabla \cdot [\theta(\rho \mathbf{V} \mathbf{V} - \boldsymbol{\sigma})] + \theta \rho \mathbf{F} \tag{13}$$

By virtue of (12) and in view of (5) and (6), the concurrent

secondary momentum balance equation of the α phase at a scale much smaller than that of the typical REV length, reads,

$$\frac{\partial}{\partial t}(\theta d^M) = -\nabla \cdot \left\{ \theta [(\mathbf{I} + \mathbf{\Omega}) \cdot d^M] \mathbf{V} \right\}, \quad \mathbf{\Omega} \equiv (\Lambda_\rho \Lambda_v)^{-1} \Lambda_{\rho v} \Lambda_v \quad (14)$$

Where, as in (12), the momentum dispersive flux $[(\rho \dot{\mathbf{v}}) \dot{\mathbf{v}}]$ is accounted for in (14). Letting the α phase represent a Newtonian fluid (i.e. its diffusive momentum flux reads $\boldsymbol{\sigma} = \boldsymbol{\tau} - P\mathbf{I}$, where P denotes pressure and the constitutive potential flow pattern for the shear stress is, $\boldsymbol{\tau} = \mu[\nabla \mathbf{v} + (\nabla \mathbf{v})^T] + \lambda \nabla \cdot \mathbf{v} \mathbf{I}$, for which μ and λ denote, respectively, the first and second viscosities), then the macroscopic Navier-Stokes equation resulting from (13) can govern the propagation of shock waves through porous media [7], conform to Forchheimer’s law accounting for the transfer of fluid inertia through the microscopic solid-fluid interface or to Darcy’s law when friction at that interface is dominant [2]. At the much smaller scale, the hyperbolic PDE of (14) describes an inertia momentum balance equation in the form of a wave equation that governs the concurrent propagation of the d^M quantity.

Spatial scaled energy balance equations of a fluid

Following Sorek et al. [4], consider a porous medium saturated by a Newtonian fluid with heat (H) as its extensive quantity ($E \equiv H$) for which its intensive quantity is $e^H \equiv C_v \rho T$ (i.e. $e^H \equiv C_v \rho$, $e^H \equiv T$) where C_v denotes the fluid constant specific heat at fixed volume, T denotes its temperature and let us also account for Γ^H denoting the specific heat source. Following Bear and Bachmat [1] and in view of (1) and (3) we obtain the fluid macroscopic heat balance equation

$$\begin{aligned} \frac{\partial}{\partial t} \left[\phi c_v (\rho T + \dot{\rho} T) \right] &= -\nabla \cdot \left[\phi c_v (\rho T + \dot{\rho} T) \mathbf{V} - \phi \mathbf{\Lambda} \cdot \nabla T \right] \\ + \phi \left[\boldsymbol{\tau} : \nabla \mathbf{V} + \boldsymbol{\tau} : (\nabla \dot{\mathbf{v}}) \right] &- \phi \frac{\beta_T}{\beta_p} \left[T \nabla \cdot \mathbf{V} + \dot{T} (\nabla \cdot \dot{\mathbf{v}}) \right] + \phi \rho \Gamma^H \end{aligned} \quad (15)$$

where ϕ denotes porosity, the fluid dispersive heat flux $c_v (\dot{\rho} T) \dot{\mathbf{v}}$ and its diffusive heat flux \mathbf{J}^H are assumed of the same order of magnitude and (following Fourier’s law, using a potential flow pattern) are assembled into $-\mathbf{\Lambda} \cdot \nabla T [= c_v (\dot{\rho} T) \dot{\mathbf{v}} + c_v \mathbf{J}^H]$ with $\mathbf{\Lambda}$ denoting the combined constant thermal dispersion and diffusion (conductance) tensor. Note that (15) accounts for the fluid viscous dissipation heat flux ($\boldsymbol{\tau} : \nabla \mathbf{V}$), although habitually considered negligible. The fluid heat flux associated with volumetric deformation $[T(\partial P / \partial T)]_v \nabla \cdot \mathbf{V}$ at fixed volume (v) is expressed in terms of the constant fluid compressibility coefficients $(\beta_T / \beta_p)_v$ with $\beta_p \equiv [(1/\rho)(\partial \rho / \partial P)]_T$ due to its pressure (P) change at fixed temperature and $\beta_T \equiv [(1/\rho)(\partial \rho / \partial T)]_P$ due to thermal change at fixed pressure. In view of (9) and (15), we obtain the primary macroscopic heat balance equation in the form

$$\frac{\partial}{\partial t}(\phi c_v \rho T) = -\nabla \cdot \left[\phi (c_v \rho T \mathbf{V} - \mathbf{\Lambda} \cdot \nabla T) \right] + \phi \boldsymbol{\tau} : \nabla \mathbf{V} - \phi \frac{\beta_T}{\beta_p} \left[T \nabla \cdot \mathbf{V} + \phi \rho \Gamma^H \right] \quad (16)$$

In view of (10) and (15), at the smaller scale, we obtain the secondary macroscopic heat balance equation in the form

$$\frac{\partial}{\partial t}(\phi d^H) = -\nabla \cdot (\phi d^H \mathbf{V}) + \phi \boldsymbol{\tau} : (\nabla \dot{\mathbf{v}}) - \phi \frac{\beta_T}{\beta_p} \left[\dot{T} (\nabla \cdot \dot{\mathbf{v}}) \right], \quad (17)$$

for which $d^H \equiv c_v \dot{\rho} T$ denotes the deviations product from the intensive heat quantity. We note that while (16) is characterised by advective and dispersive heat transfer, concurrent at the smaller scale (17) addresses pure advective flux of heat transfer.

Spatial scaled component mass balance equations in a fluid

In Sorek and Ronen [3] we consider a γ component for

which m^γ denotes its mass so its extensive quantity is $E \equiv m^\gamma$ with the intensive quantity ($e^{m^\gamma} \equiv C = \rho \omega$) given by its concentration $C (= e_1^{m^\gamma} e_2^{m^\gamma}; e_1^{m^\gamma} \equiv \omega, e_2^{m^\gamma} \equiv \rho)$ related to its mass fraction (ω), and let us account for the specific component source (Γ^{m^γ}). Let us consider a saturated domain, following Fick’s law based on a potential flow pattern we combine the component diffusive flux vector (\mathbf{J}^{m^γ}) and its dispersive flux vector $\dot{C} \dot{\mathbf{v}} [= (\rho \omega) \dot{\mathbf{v}}]$ into $-\mathbf{D}_h \cdot \nabla C (= \dot{C} \dot{\mathbf{v}} + \mathbf{J}^{m^\gamma})$ for which \mathbf{D}_h denotes a hydrodynamic dispersion tensor. In view of (9), at the REV spatial scale we obtain the primary component mass balance equation in the form

$$\frac{\partial}{\partial t}(\phi C) = -\nabla \cdot [\phi (C \mathbf{V} - \mathbf{D}_h \cdot \nabla C)] + \phi \rho \Gamma^{m^\gamma} \quad (18)$$

We note that (18) describes the transport of a component subject to advective and dispersive flux mechanisms, interpreted by hyperbolic and parabolic PDE characteristics, respectively.

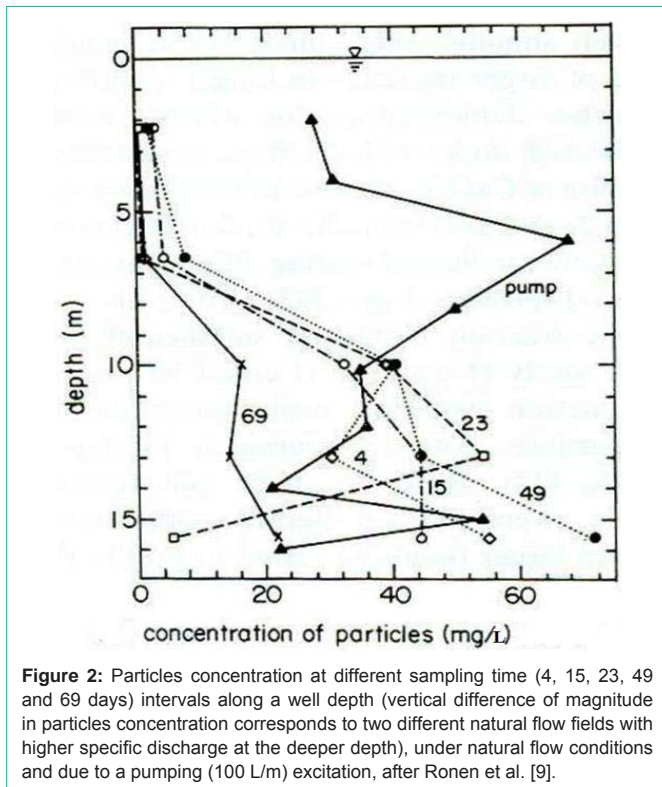
In view of (10), at the smaller scale, the secondary component mass balance equation becomes

$$\frac{\partial}{\partial t}(\phi d^{m^\gamma}) = -\nabla \cdot (\phi d^{m^\gamma} \mathbf{V}), \quad (19)$$

where $d^{m^\gamma} (= \dot{\omega} \dot{\rho})$ denotes the deviations product from the component concentration. We note that concurrent to the advective dispersive transport described by (18), the transport at the adjacent scale, significantly smaller than that of the REV typical length, is governed by (19) which describes a pure advection mechanism.

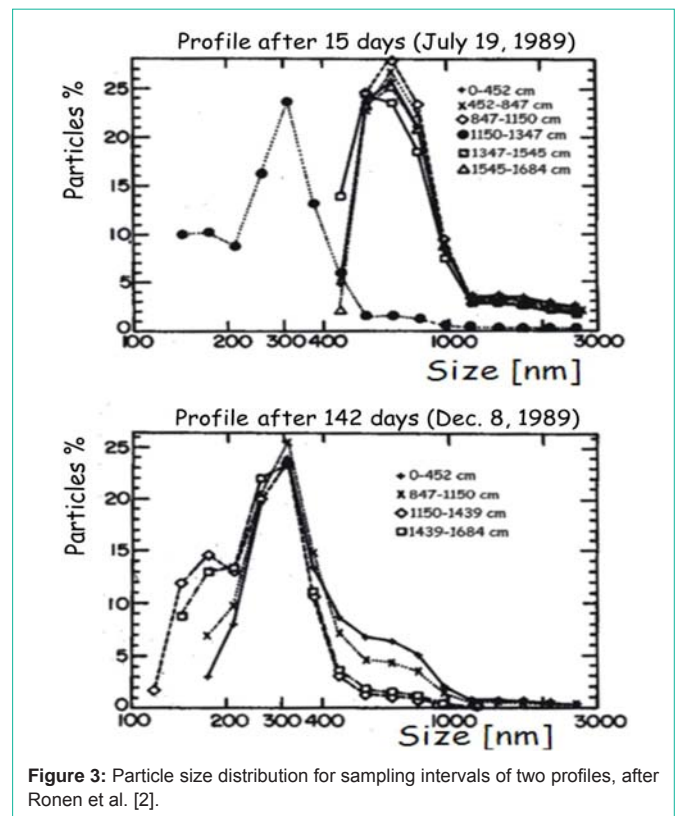
Supporting observations of particles migration at the scale of several pores

We note that the form of macroscopic balance equations at the smaller (e.g. several pores) scale is proven to be hyperbolic PDE’s. This suggests a “bulk flow” phenomenon, at that scale, of moving particles aggregated by a shock wave drive. We suggest that this “bulk flow” mechanism is governed by a wave equation for the fluid momentum balance equation and pure advection transport for the particle’s mass balance equation. Numerical predictions or simulations addressing a sensitivity analysis cannot alter the basic characteristics of the balance hyperbolic PDEs at the smaller scale. We thus maintain that validation of the theoretical development should at first rely on verifying that observations at the several pores scale comply with features of the theoretical model at that scale. Field observations under natural gradient flow conditions (specific discharge of 4 to 16/myr and 35% porosity) in a contaminated sandy aquifer show, micro-scale variations in the flux, mineralogical composition and size of suspended particles [9,10]. Along a 16 m saturated section below the water table the average concentration of particles in groundwater varied between 1 and 40 mg/L, but high concentrations of up to 5000 mg/L were also detected. The particles were composed of CaCO₃ (11-57%), quartz (7-39%) and clays (8-43%). Most of the particles were within the 140-3000 nm size range with size modes varying from 310-660 nm. The transport of large amounts of particles under the above mentioned natural flow conditions within a porous medium (average grain size of 125 nm) is striking. Motion of different particle parcels observed along the depth of a well and sampled at different time periods, under natural flow conditions and due to a sudden single pumping excitation (100 L/mm), are depicted in Figure 2. We note in Figure 2 that the single pumping caused the rise of colloids turbidity



(a measure of the degree to which a fluid loses its transparency due to the presence of suspended particles). This can be explained in view of (13) concerning temporal scaling (explained in the following section 3) for the large spatial scale of a fluid momentum saturating a porous matrix [11], confirmed by simulation of its simplified form [12] and validated through different experiments [13]. In view of these [11-13], we maintain that at the start of pumping, inertia temporally governs the flow regime and a wave driven transport at that instant caused the rise of colloids turbidity (Figure 2). At the several pores scale, (14) and (19) suggest that displacement be governed by the combination of wave influenced motion and pure advective transport mechanisms, respectively. The several pores scale motion of condensed parcels of particles that complies with the hyperbolic forms of (14) and (19), is also demonstrated in Figure 2. Vertical difference of magnitude in particles concentration (Figure 2) corresponds to two different natural flow fields reflecting a higher specific discharge at the deeper depth and thus transporting significantly more particles at that depth [9].

At the several pores scale, (14) and (19) suggest that displacement be governed by the combination of wave influenced motion and pure advective transport mechanisms, respectively. Motion of fronts (observed as continuous bulk displacement or “piston flow”) remaining sharp, is a characteristic solution of hyperbolic PDEs. The motion of condensed parcels of particles exhibited in Figure 2, noticeably complies with the typical solution featured by the hyperbolic forms of (14) and (19). Hence, we maintain that observations depicted in Figure 2 validate that the PDEs of (14) and (19) govern the hydrodynamics at the scale of several pores. Vertical difference of magnitude in parcels of particles concentration (Figure 2) corresponds to two different natural flow fields reflecting



a higher specific discharge at the deeper depth and thus displacing significantly more particles at that depth [9]. At the pores scale and for two time snapshots, Figure 3 depicts bulk motion of dominant mean size (determined by their weight percentage) particles along depth. Observations depicted in Figure 3 thus attest by the mass bulk displacements, the hydrodynamics of wave influenced motion and pure advective transport resulting from the hyperbolic PDEs of (14) and (19), respectively.

Temporal Scaling of the Transport Phenomena through Porous Media

In what follows we neglect the secondary balance equations of the fluid momentum (14) and (19) the component mass. Actually, such a decision leans towards a qualitative rather than a quantitative premise. The resolution of the relative influence between the smaller and bigger spatial scales should rely on quantitative (e.g. numerical exercises) measures and be investigated thoroughly. We thus consider as dominant the macroscopic balance equations of the fluid momentum (13) in the form of the NS equation and refer to (18) for the mass balance equation of a γ component.

In Sorek et al. [11] we further develop the time evolving approximate forms of these balance equations, after an abrupt rise of the fluid pressure. We consider linear equilibrium adsorption isotherm, deformable saturated porous matrix and a varying fluid density $\rho = \rho(P, C)$. On the basis of dimensional analysis we find [11] that the balance equations of the fluid momentum and mass and the component mass, conform to different dominant forms as time evolves after the onset of the abrupt pressure rise. We will specifically draw our attention to the first two evolution periods as well as summarize aspects presented in [11].

Considering a fluid without mass source, without diffusion and dispersion fluxes of its mass (i.e. $E \equiv m, e^m = \rho, \Gamma^m = 0, \rho \dot{\mathbf{V}} = 0, \mathbf{J}^m = 0$), then in view of (11) we write the *fluid mass balance equation* in the form

$$\frac{\partial}{\partial t}(\phi \rho) = -\nabla \cdot (\phi \rho \mathbf{V}) \tag{20}$$

Following (13) we obtain the *fluid momentum balance equation* in the form [14]

$$\phi \rho \left(\frac{\partial \mathbf{V}}{\partial t} + \mathbf{V} \cdot \nabla \mathbf{V} \right) = -\phi (\nabla P + \rho \mathbf{g} \nabla Z) \cdot \mathbf{T}^* + (\mu + \lambda) \nabla \nabla \cdot \mathbf{q}_f + \mu (\nabla^2 \mathbf{q}_f - \frac{c_f}{\Delta^2} \alpha' \cdot \mathbf{q}_f) \tag{21}$$

where \mathbf{g} denotes gravity acceleration, Z denotes altitude, $\mathbf{q}_f [\equiv \phi (\mathbf{V} - \mathbf{V}_s)]$ denotes the specific fluid flux vector relative to (\mathbf{V}_s) the solid phase velocity vector, c_f denotes a shape factor, Δ denotes the hydraulic radius of the pore space and $\alpha'_{ij} [\equiv (1/S_{fs}) \int (\delta_{ij} - \xi_i \xi_j) dS]$ denotes the ij components of a cosine direction tensor at the microscopic S_{fs} fluid-solid interface, and δ denotes the Kronecker delta tensor. Sorek et al. [2] extend the macroscopic NS equation of (21) when, by virtue of (21), ∇P through S_{fs} is replaced with all of the microscopic NS equation flux terms $(\int_{S_{fs}} \hat{x}_i (\partial P / \partial x_i) \xi_j dS = \int_{S_{fs}} \hat{x}_i \rho (\partial V_j / \partial t + V_j \partial V_i / \partial x_i) + \rho g \hat{z} / \partial x_i - \partial \tau_i / \partial x_i \xi_j dS)$. Subject to some assumptions, Sorek et al. [2] obtain an *extended macroscopic NS equation* that reads

$$\phi \rho \left(\frac{\partial \mathbf{V}}{\partial t} + \mathbf{V} \cdot \nabla \mathbf{V} \right) \equiv -\phi (\nabla P + \rho \mathbf{g} \nabla Z) \cdot \mathbf{T}^* - \frac{c_f}{2\Delta^2} \phi \rho |\mathbf{V}| \mathbf{V} \cdot \tilde{\mathbf{F}} - \mu \phi \frac{c_f}{\Delta^2} \alpha' \cdot \mathbf{V} \tag{22}$$

In which $\tilde{F}_{ij} [\equiv (\frac{1}{S_{fs}}) \int_{S_{fs}} \hat{x}_i (\delta_{ij} - \xi_i \xi_j) dS]$ denotes the kji components of the Forchheimer 3rd rank tensor. For a fully developed flow regime [i.e. $\phi \rho (\partial \mathbf{V} / \partial t + \mathbf{V} \cdot \nabla \mathbf{V}) \ll \mu \phi (c_f / \Delta^2) \alpha' \cdot \mathbf{V}$] (22) reduces to Forchheimer Law which together with the assumption of a Reynolds number less than a unit (22) reduces to Darcy's Law [2]. Note that it is based on rigors macroscopic continuum mechanic approach such that at a point (i.e. within the REV) there is an account for the interaction of at least two phases also through their common microscopic interface. Thus, e.g., Darcy's Law was proven [2] to be a derivative of the macroscopic NS momentum balance equation which validated the originally suggested empirical relation for flow through a porous medium bulk. One can, however, find microscopic derivation of the equivalent to Darcy's Law when it is considered as a phenomenological filtration relation for, say, membrane technology [15].

Following an abrupt up-rise of pressure, the investigation for the approximate forms of the balance equations will be sought in terms of pressure rate, which can be obtained from the differentiations of $\rho = \rho(P, C)$. Hence, (21) will be substituted by a combined form of (20) and (21). Considering no mass source for the component and by virtue of (9), we write the component mass balance equation in the fluid accounting also for its adsorption on the solid matrix, i.e. the *component transport equation*, in the form

$$\frac{\partial}{\partial t} [\phi C + (1 - \phi) C_s] = -\nabla \cdot [\phi (C \mathbf{V} - \mathbf{D}_h \cdot \nabla C)], \tag{23}$$

in which $C_s (= \rho_s k_d C)$; where ρ_s denotes the solid density and k_d denotes the partitioning coefficient) denotes the component mass per unit volume of solid matrix. Analyzing (23) in orders of the pressure rate magnitude during different time scales, we assume a low solubility (i.e. concentration is practically sought in terms of the fluid volume) and that changes in the total stress of the porous matrix are of the same order as pressure (i.e. $\phi = \phi(P)$). To address the transport phenomena during different time scales [11] we will analyze the

order of magnitude of the terms appearing in the balance equations set (20), (21) and (23). This set is thus rewritten in nondimensional forms obtained by subdividing all terms by the one associated with the pressure rate.

At the first time $t_1 (= 0^+)$ being the onset instant of the abrupt pressure rise, starting with fluid at rest with no loss of generality, we have $t_1 = t_1^p = t_1^v = t_1^c$; $L_c^p \equiv L_c^v \equiv L_c^c$. Where $()_c$ denotes a characteristic quantity, and the characteristic velocity $V_c^e \equiv L_c^e / t_c^e$ thus becomes $V_c^p = V_c^v = V_c^c = V_c$ resulting in a Strouhal number being $St^e \equiv \frac{L_c^e / t_c^e}{V_c} = 1$.

Following Sorek [11] at t_1 the first time scale addressing the up-rise of the pressure impulse, we obtain:

The *fluid mass balance equation* conforming to

$$\frac{DP}{Dt} = 0, \tag{24}$$

and the *fluid momentum balance equation* reads

$$\phi \nabla P \cdot \mathbf{T}^* = 0 \tag{25}$$

Assuming that adsorption is a slow process in comparison to change in pressure rate such that it does not affect the component mass, the *component transport equation* becomes

$$(1 - \phi) \beta_\phi C \frac{DP}{Dt} = 0, \tag{26}$$

where $\beta_\phi \{ = -(1/\phi) [\partial(1 - \phi) / \partial P] \}$ denotes the matrix compressibility and $D/Dt (\equiv \partial / \partial t + \mathbf{V} \cdot \nabla)$ denotes the hydrodynamic time derivative operator. By virtue of (24) and (25) the magnitude of the pressure rise will propagate without attenuation ($P|_{t=0^+} = Const.$) as if through an incompressible fluid, and (26) is automatically fulfilled. On the basis of the dimensional analysis the order of magnitude for the pressure propagation distance will be $L_1 = O(t_1 \sqrt{\phi_c / (\rho_s S_0)})$,

for which $s_0 [\equiv \phi \beta_\phi + (1 - \phi) \beta_s]$ denotes the specific storativity of the porous medium.

At the second consecutive evolution time t_2 period, we have $t_2 = t_2^p = t_2^v = t_2^c$; $L_c^p > L_c^v \cong L_c^c$ leading to, $V_c^p > V_c^v = V_c^c = V_c$, however the velocity Strouhal number ($St^v=1$) remains as was at the first time scale. It is proven Sorek [11] that at this second time scale the fluid mass balance equation is described by (20) while the *fluid momentum balance equation* conforms to a non-linear wave equation that reads,

$$\frac{D\mathbf{V}}{Dt} + \left(\frac{\nabla P}{\rho} + \mathbf{g} \nabla Z \right) \cdot \mathbf{T}^* = 0 \tag{27}$$

The dimensional analysis asserts that the non-linear wave in the form of (27) prevails during an order of time magnitude being $t_2 = O(P_c / (\rho_c V_c g))$, and the order of magnitudes of the characteristic pressure ($P_c > \rho_c V_c^2$) with $L_2 = O(P_c / \rho g)$ as its propagation distance.

We note from the dimensional analysis [11] that during the time period starting at t_2 , the solution for P and \mathbf{V} of (27) can be obtained separately with no reference to the solution of the component concentration, as during time increments resolving for the evolution of P and \mathbf{V} of (27) we have $\rho \cong \rho(P)$. The update, by the end of each time increment, of fluid density associated with component concentration ($\rho = \rho(P, C)$) will be after solving for the component transport equation.

The component transport equation becomes,

$$\frac{1}{C} \frac{DC}{Dt} = - \left(\frac{1-\phi}{\phi} \right) \beta_g \rho_s \kappa_d \mathbf{V} \cdot \nabla P - \frac{\phi \beta_p + \rho_s \kappa_d S_0}{S_0} \nabla \cdot \mathbf{V} \quad (28)$$

Hence, the pre-evaluation of P and \mathbf{V} can be interpreted in (28) as known source terms. The dimensional analysis suggests that the order of magnitude of the component concentration spatial distribution will be to a distance $L_{2c} = \theta(V_c^2/g)$.

Levi-Hevroni et al. [16] apply a dimensional analysis accounting for the fluid momentum in the form of (22) to investigate the wave period starting at t_2 (following an abrupt change in fluid's pressure and temperature) for the fluid heat transfer and flow problem, and solid deformation concerning a thermoelastic highly flexible porous matrix. We note in Figure 4 that the 1-D numerical simulation conducted by Levi-Hevroni et al. [16] yield excellent agreement with 1-D numerical simulation for almost non-deformable porous materials Levy et al. [17] and with shock-tube experimental observations Levy et al. [18] for the pressure histories of air at various locations along the shock wave propagation pass. The contact surface of the gas which originally filled

the pores and was pushed out, was found experimentally by Skews et al. [19] and reported in Levi-Hevroni et al. [16] to be reproduced numerically. The calculated gas density field and the trajectory of the foam front edge are depicted in Figure 5.

Burde and Sorek [12] investigated the component transport during the wave period starting at the second time scale t_2 . A simplified analytical solution is applied for the 1-D case of the set (20), (27) and (28) where the flow problem is addressed by the traveling wave (kinematic wave) case (Landau and Lifshitz, 1987) for which $V=V(\rho)$; $P=P(\rho)$ and thus the fluid mass and momentum balance equations are rewritten in a similar wave equation form in terms of V or P . The solid matrix is considered as slightly deformable following the assumption that $\partial\phi/\partial t \gg V_s \partial\phi/\partial x$, in which $()_s$ denotes a quantity associated with the solid porous matrix. Component migration Burde and Sorek [12] due to the action of a compaction wave (e.g. change in injection rate) or an expansion wave (e.g. change in pumping rate), both when being emitted at the surface ($x=0$), are depicted in Figure 6. Solutions Burde and Sorek [12] are presented as time evolves from t_2 , and the component displacement is continuously governed by the wave form of (27).

Simulations findings of Burde and Sorek [12] for migration of a component governed by continuous propagation of a shock wave, was verified to be consistent with solutes displacements observed through various experimental setups under the action of emitting a succession of compaction waves [13].

Further for a deformable matrix, during the compaction wave period at the second time increment, on top of the fluid mass (20) and momentum (22) balance equations the solid mass and momentum balance equations read respectively [21].

$$\frac{\partial}{\partial t} [(1-\phi)\rho_s] + \nabla \cdot [(1-\phi)\rho_s \mathbf{V}_s] = 0, \quad (29)$$

$$\frac{\partial}{\partial t} [(1-\phi)\rho_s \mathbf{V}_s] + \nabla \cdot [(1-\phi)\rho_s \mathbf{V}_s \mathbf{V}_s] + (1-\phi)\nabla P \cdot \mathbf{T}_s^* - \nabla \cdot \hat{\sigma}'_s - \frac{c_f}{2\Delta^2} \phi \rho |\mathbf{V}| \mathbf{V} \cdot \bar{\mathbf{F}} = 0,$$

$$\sigma'_s = (1-\phi)(\sigma_s - \sigma_f), \quad (30)$$

where σ'_s ($\alpha = f, S$) denotes the α phase stress tensor with σ'_s as the matrix effective stress, and the phases tortuosity tensors are related by $\phi \mathbf{T}^* + (1-\phi)\mathbf{T}_s^* = \boldsymbol{\delta}$. Considering an elastic matrix undergoing deformations we refer to a constitutive relation for σ'_s s equivalent to the microscopic Hooks law, and a strain tensor e_s that read,

$$\sigma'_s = \lambda'_s \nabla \mathbf{w}_s \mathbf{I} + 2\mu'_s e_s, \quad e_s = \frac{1}{2} [\nabla \mathbf{w}_s + (\nabla \mathbf{w}_s)^T], \quad (31)$$

where μ'_s denotes the macroscopic Lamé constant related to the matrix shear strain, \mathbf{I} denotes the unit tensor and \mathbf{w}_s denotes the matrix displacement vector. Referring to the set of fluid, (20), (22) and matrix (29) - (31) mass and momentum balance equations together with the solute mass balance (23) equation, the 1D component displacement due to compaction waves propagation are solved numerically using the Total Variation Diminishing (TVD) scheme [21]. Solute extraction is simulated in view of applying at the medium surface a sequence of pressure pulses each generating an expansion wave. The inwards expansion wave generates a pressure gradient contradicting the direction of the wave propagation. The fluid flow governed by the pressure gradient, will thus displace the component towards

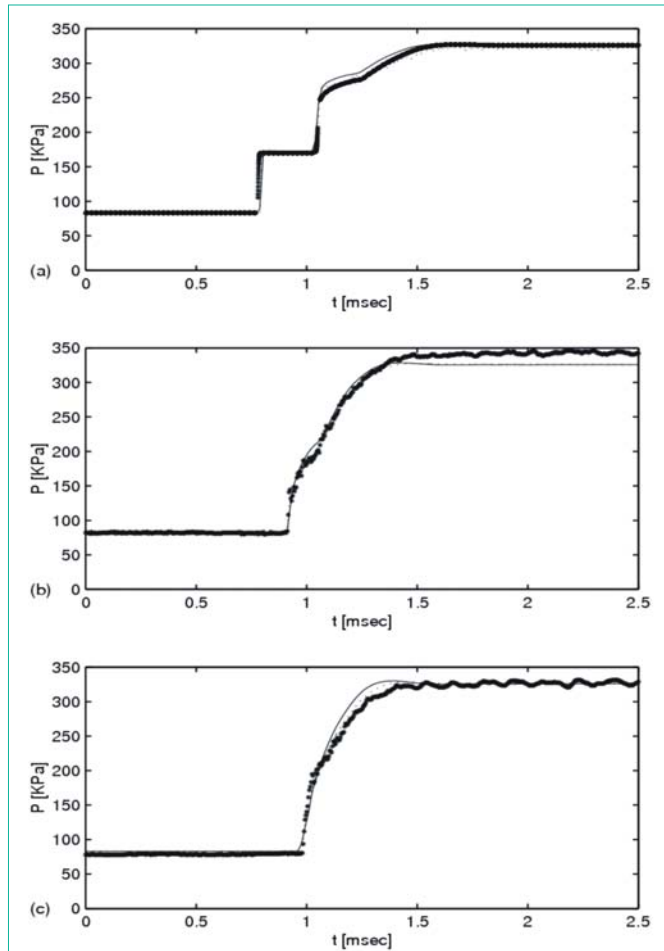


Figure 4: Experimental results and numerical predictions [dotted line - Levy et al. [17] and solid line - Levi-Hevroni et al. [16] of the gas pressure histories (after Levi-Hevroni et al. [16] using a 40 mm long silicon carbide sample with 10 pores/Inch and average porosity of 0.728 ± 0.016 . Incident-shock wave Mach number in this experiment was $M_s = 1.378$. (a) Upstream 43 mm ahead the porous material front edge. (b) Along the shock tube side-wall inside the porous material, 23 mm from end-wall. (c) At the shock tube end-wall.

the medium surface. Using such a procedure [21] the component's mass extraction is compared between pumping and application of expansion waves emitted from the surface. Pumping refers to Darcy's law for which drag is assumed dominant at the solid-fluid interface, neglecting gravitational body force, the matrix momentum balance equation (30) is assumed static and (31) accounts for its stress constitutive law. (Sorek and Ohana, 2009) develop an approximate analytical solution for the specific component's extraction mass flux $Q_{solute-p}$ for constant pumping intensity at the surface. Their comparison (Table 1) with $Q_{solute-w}$ for specific solute extraction mass flux due to emitting expansion waves proves the overwhelming advantage of the latter.

Bear and Sorek [5] discuss two additional forms of dominant governing fluid mass and momentum balance equations due to the onset of an abrupt pressure rise. Following the first two aforementioned evolution periods, at the start of the third ascending time scale, fluid's inertial and drag momentum fluxes are of the same order expressed by the full extent of NS equation that can also conform to Forchheimer Law [2]. During the fourth evolution time period, drag associated with viscosity dominates the flow regime and inertial momentum flux becomes negligible in comparison. The resulting viscous creep flow is expressed by the Brinkman momentum equation, when friction between two adjacent fluid layers dominates, or by Darcy's linear momentum, when friction at the solid-fluid interface dominates [2].

Conclusion

The macroscopic balance equations describing the transport phenomena through porous media are spatial and temporal dependent. Space wise each balance equation is decoupled into a primary equation addressing the REV length span scale and a secondary equation, concurrent to the primary one, valid at a length scale smaller than that of the REV. The latter is associated with intensive quantities deviating from their corresponding averaged

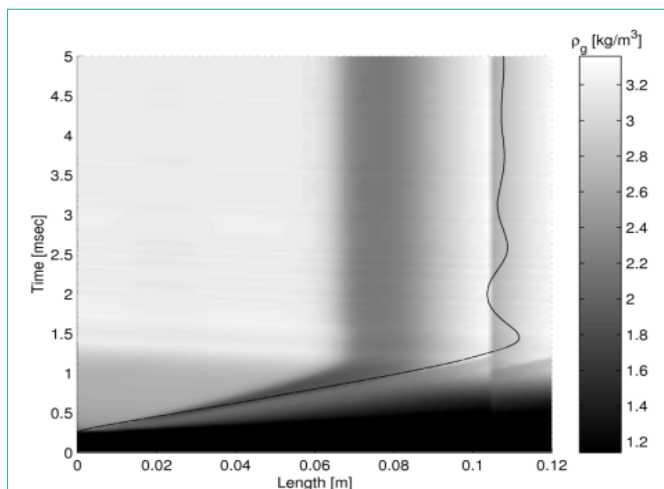


Figure 5: Calculated gas density field and front edge trajectory of the flexible elasto-plastic porous sample (after Levi-Hevroni et al. [12]). We note the contact surface due to gas emerging from the sample porous matrix, after it had reached its utmost deformation. This very large deformation depleted the sample pores and forced the gas to flow across the sample/gas interface. Simulation results are similar to the experimental observations of Skews et al. [19].

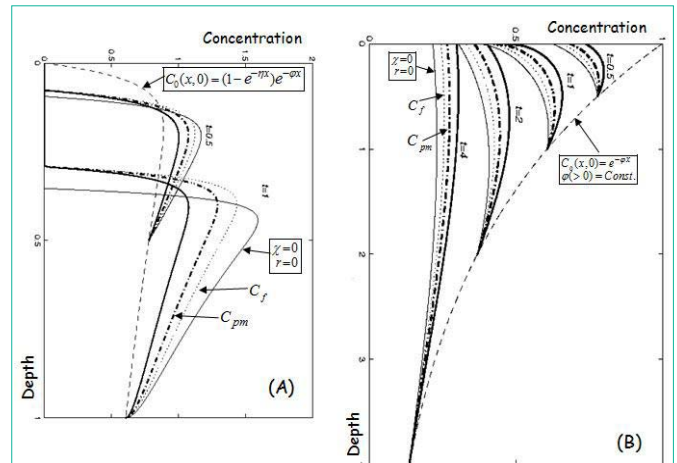


Figure 6: 1-D simulations, for a general unit system, of a component migration through a saturated porous medium, as time evolves starting at the second time scale following an abrupt up-rise of pressure Burde and Sorek [12]. With $()_0$ that denotes a value at the reference $x=0, t=0$, solutions are also depicted in terms of $C_f \equiv (\phi/\phi_0) C \left[\frac{\text{(component's mass in the fluid)/(unit volume of porous m.)}}{\text{(same values at the reference } x=0, t=0)}, of $\chi \equiv \rho_s k_d$ that addresses a measure of adsorption, of $r \equiv (1 - \phi_0)/\lambda_s \rho_0 T^*$ that provides a measure of the matrix stiffness (λ_s denotes the Lamé coefficient, analogous to Young's elastic modulus of Hooks law), and for values of $C_{pm} \equiv \frac{\phi + \chi(1 - \phi)}{\phi_0 + \chi(1 - \phi_0)} C \left[\frac{\text{(component's mass in the p. m.)/(unit volume of p. m.)}}{\text{(same values at the reference } x=0, t=0)}. Waves are being emitted at the surface ($x=0$), with $C_0(x,0)$ denoting the initial concentration distribution and for $\chi = 0.25, r = 0.25$. (A) Temporal concentration along depth under the action of continuous propagation of a compaction wave. (B) Temporal mass extraction subject to the action of continuous expansion wave propagation.$$

terms. The primary balance equation can conform to a pure hyperbolic PDE addressing advective fluxes, PDE with hyperbolic-parabolic characteristics expressing advective-diffusive (with/without dispersive) fluxes or pure parabolic PDE governing diffusive (with/without dispersive) flux mechanisms. The secondary balance equation remains a pure hyperbolic PDE for any extensive quantity of a phase or component. The secondary macroscopic balance equations are habitually neglected, yet these can be significant in cases of deviation from the average fluid velocities and/or for heterogeneity in fluid and matrix properties. Validation of the theoretical development relies on verifying that field observations under natural gradient flow conditions indicate that particles are displaced in parcels at several pores scale and thus comply with features of the mass and momentum balances at that scale.

Approximate macroscopic mass and Navier-Stokes fluid balance equations and the component mass balance equation through different time scales were developed following the onset of an abrupt pressure change. Numerical simulations were consistent and in excellent agreement with experimental observations.

Table 1: Values of $Q_{solute-p}/Q_{solute-w}$ for typical matrix properties.

	Depth[m]	Pervious	Semi-Pervious	Impervious
		Sand & Gravel; Fractured Rocks	Silt; Loess; Layered clay; Oil Reservoir Rocks	Unweathered clay; Limestone; Dolomite
Water	30	0.06	5.0*E-05 to 5.0*E-07	5.0*E-09
Air	10	0.002	2.0*E-06 to 2.0*E-08	2.0*E-10

References

1. Bear J, Bachmat Y. Introduction to Modeling of Transport Phenomena in Porous Media, Kluwer Academic Publishers, Dordrecht, The Netherlands. 1990.
2. Sorek S, Levi-Hevroni D, Levy A, Ben-Dor G. Extensions to the Macroscopic Navier-Stokes Equation, *Transport in Porous Media*. 2005; 61: 215-233.
3. Sorek S, Ronen D. Scale dependent fluid momentum and solute mass macroscopic balance equations: Theory and observations, *CMWR XVI*, Copenhagen, Denmark, 2006.
4. Sorek S, Ronen D, Gitis V. Scale-dependent Macroscopic Balance Equations Governing Transport through Porous Media: Theory and Observations, *Transport in Porous Media*. 2010; 81: 61-72.
5. Bear J, Sorek S. Evolution of Governing Mass and Momentum Balances Following an Abrupt Pressure Impact in a Porous Medium. *Transport in Porous Media*. 1990; 5: 169-185.
6. Sorek S, Bear J, Ben-Dor G, Mazor G. Shock Waves in Saturated thermoelastic Porous Media, *Transport in Porous Media*. 1992; 9: 3-13.
7. Levy A, Sorek S, Ben-Dor G, Bear J. Evolution of the balance equations in saturated thermoelastic porous media following abrupt simultaneous changes in pressure and Temperature, *Transport in Porous Media*. 1995; 21: 241-268.
8. Levy A, Levi-Hevroni D, Sorek S, Ben-Dor G. Derivation of Forchheimer Terms and their Verification by Application to Waves Propagation in Porous Media. *Intl J MultiPhase Flow*. 1999; 25: 683-704.
9. Ronen D, M Magaritz U, Weber AJ, Amiel, E Klein. Characterization of suspended particles collected in groundwater under natural gradient flow conditions, *Water Resources Research*. 1992; 28: 1279-1291.
10. Weisbrod N, Ronen D, Nativ R. A new method for sampling groundwater colloids under natural gradient flow conditions, *Environmental Science & Technology*. 1996; 30: 3094-3101.
11. Sorek S. A model for solute transport following an abrupt pressure impact in saturated porous media, *Transport in Porous Media*. 1996; 22: 271-285.
12. Burde GI, Sorek S. Solute transport in variable density regime, following an abrupt pressure change in saturated porous media: A simple analytical solution}, Bentley LR, Sykes JF, Brebbia CA, Gray WG. GF Pinder (eds), *Computational Methods in Water Resources*, Proc. of the XIII Int. Conf. 2000; 1: 339-344.
13. Gross A, Besov A, Reck DD, Sorek S, Ben-Dor G, Britan A, et.al . Application of waves for remediation of contaminated aquifers. *Environ Sci Technol*. 2003; 37: 4481-4486.
14. Bear J, Bachmat Y. Macroscopic modeling of transport phenomena in porous media 2: Applications to mass, momentum and energy transport. *Transport in Porous Media*. 1986; 1: 241-270.
15. Gladkov SO. Microscopic Derivation of Darcy's Law. *Russian Physics Journal*. 1998; 41: 969-974.
16. Levi-Hevroni D, Levy A, Ben-Dor g, Sorek S. Numerical Investigation of the Propagation of Planar Shock Waves in Saturated Flexible Porous Materials: Development of the Computer Code and Comparison with Experimental Results. *J Fluid Mech*. 2002: 462, 285-306.
17. Levy A, Ben-Dor G, Sorek S. Numerical investigation of the propagation of shock waves in rigid porous materials: development of the computer code and comparison with experimental results. *J Fluid Mech*. 1996; 324: 163-179.
18. Levy A, Ben-Dor G, Skwes S, Sorek S. Head-on collision of normal shock waves with rigid porous materials, *Exp Fluids*. 1993; 15: 183-190.
19. Skews BW, Atkins MD, Seitz MW. The impact of shock wave on porous compressible foams. *J Fluid Mech*. 1993; 253: 245-265.
20. Landau LD, Lifshitz EM. *Fluid Mechanics*, England, Pergamon Press. 1987.
21. Sorek S, Ohana Y. Shock Wave through Deformable Saturated Porous Media, *Poromechanics IV*, Fourth Biot Conf. on Poromechanics, HI Ling, A Smyth, R Betti, editors. Columbia NY, USA, 2009; 31-42.